

RESEARCH ARTICLE

Myocardial Mitochondrial and Contractile Function Are Preserved in Mice Lacking Adiponectin

Martin Braun¹, Niko Hettinger¹, Christoph Koentges¹, Katharina Pfeil¹, Maria C. Cimolai¹, Michael M. Hoffmann^{1,3}, Moritz Osterholt², Torsten Doenst², Christoph Bode¹, Heiko Bugger^{1*}

1 Division of Cardiology and Angiology I, Heart Center Freiburg University, Freiburg, Germany, **2** Department of Cardiothoracic Surgery, Jena University Hospital, Jena, Germany, **3** Institute for Clinical Chemistry and Laboratory Medicine, Freiburg University Hospital, Freiburg, Germany

* heiko.bugger@universitaets-herzzentrum.de



Abstract

Adiponectin deficiency leads to increased myocardial infarct size following ischemia reperfusion and to exaggerated cardiac hypertrophy following pressure overload, entities that are causally linked to mitochondrial dysfunction. In skeletal muscle, lack of adiponectin results in impaired mitochondrial function. Thus, it was our objective to investigate whether adiponectin deficiency impairs mitochondrial energetics in the heart. At 8 weeks of age, heart weight-to-body weight ratios were not different between adiponectin knockout (ADQ^{-/-}) mice and wildtypes (WT). In isolated working hearts, cardiac output, aortic developed pressure and cardiac power were preserved in ADQ^{-/-} mice. Rates of fatty acid oxidation, glucose oxidation and glycolysis were unchanged between groups. While myocardial oxygen consumption was slightly reduced (-24%) in ADQ^{-/-} mice in isolated working hearts, rates of maximal ADP-stimulated mitochondrial oxygen consumption and ATP synthesis in sapo-nin-permeabilized cardiac fibers were preserved in ADQ^{-/-} mice with glutamate, pyruvate or palmitoyl-carnitine as a substrate. In addition, enzymatic activity of respiratory complexes I and II was unchanged between groups. Phosphorylation of AMP-activated protein kinase and SIRT1 activity were not decreased, expression and acetylation of PGC-1 α were unchanged, and mitochondrial content of OXPHOS subunits was not decreased in ADQ^{-/-} mice. Finally, increasing energy demands due to prolonged subcutaneous infusion of isoproterenol did not differentially affect cardiac contractility or mitochondrial function in ADQ^{-/-} mice compared to WT. Thus, mitochondrial and contractile function are preserved in hearts of mice lacking adiponectin, suggesting that adiponectin may be expendable in the regulation of mitochondrial energetics and contractile function in the heart under non-pathological conditions.

OPEN ACCESS

Citation: Braun M, Hettinger N, Koentges C, Pfeil K, Cimolai MC, Hoffmann MM, et al. (2015) Myocardial Mitochondrial and Contractile Function Are Preserved in Mice Lacking Adiponectin. PLoS ONE 10(3): e0119416. doi:10.1371/journal.pone.0119416

Academic Editor: Luc Bertrand, Université catholique de Louvain, BELGIUM

Received: September 6, 2014

Accepted: January 13, 2015

Published: March 18, 2015

Copyright: © 2015 Braun et al. This is an open access article distributed under the terms of the [Creative Commons Attribution License](https://creativecommons.org/licenses/by/4.0/), which permits unrestricted use, distribution, and reproduction in any medium, provided the original author and source are credited.

Data Availability Statement: All relevant data are within the paper and its Supporting Information files.

Funding: The authors received no specific funding for this work.

Competing Interests: The authors have declared that no competing interests exist.

Introduction

Adiponectin is an adipose tissue-derived cytokine which is abundantly present in human plasma [1]. Adiponectin exerts pleiotropic effects on its target tissues, including regulation of cellular energy metabolism. Adiponectin is able to increase glucose uptake and fatty acid oxidation in skeletal muscle, and to suppress glucose production and to decrease lipid content in the liver [2–4]. In mice, adiponectin deficiency is associated with insulin resistance, low mitochondrial content and reduced mitochondrial enzyme activity in skeletal muscle [5]. Conversely, adiponectin treatment of human myotubes in primary culture induces mitochondrial biogenesis, palmitate oxidation, and citrate synthase activity [5]. Finally, Iwabu and colleagues demonstrated that adiponectin is capable of activating peroxisome proliferator-activated receptor γ coactivator 1 α (PGC-1 α) signaling and mitochondrial biogenesis by activating Ca²⁺/calmodulin-dependent protein kinase kinase b (CaMKKb), or by activating the AMP-activated protein kinase (AMPK)/sirtuin 1 (SIRT1) signaling cascade in skeletal muscle [6]. Thus, adiponectin regulates cellular energy metabolism, including mitochondrial biogenesis and energetics.

The heart is highly dependent on continuous ATP delivery from mitochondrial substrate oxidation to main cardiac pump function. Impairment in mitochondrial function is observed in numerous cardiac pathologies, including the diabetic and the failing heart [7,8]. Mitochondrial dysfunction is also a major determinant of myocardial injury following ischemia-reperfusion [9]. Serum adiponectin levels are lower in patients with clinical manifestations of coronary artery disease, and adiponectin deficiency in mice leads to increased myocardial infarct size following ischemia reperfusion [10,11]. A decrease in serum adiponectin levels is associated with progression of left ventricular hypertrophy with diastolic dysfunction, and adiponectin deficiency in mice exaggerates cardiac hypertrophy following pressure overload [12,13]. While the mechanisms of increased infarct size or increased hypertrophy in adiponectin deficiency have been related to AMPK- and cyclooxygenase-2 (COX-2)-dependent mechanisms or activation of extracellular-signal regulated kinase (ERK), respectively, a possible contribution of mitochondrial dysfunction has not been investigated in detail to date. We hypothesize that adiponectin deficiency may impair myocardial mitochondrial function, which may potentially promote adverse cardiac outcomes following ischemia-reperfusion or pressure overload. Thus, it was our objective to investigate whether adiponectin deficiency impairs mitochondrial function in the heart.

Methods

Animals

Male adiponectin knockout mice (ADQ^{-/-}) and respective C57BL/6J wildtype (WT) littermate controls were purchased from The Jackson Laboratories (Bar Harbor, ME) and studied at the age of 8 weeks. Animals were housed at 22°C with a 12-hour light/12-hour dark cycle with free access to water and standard chow. The study conforms to the *Guide for the Care and Use of Laboratory Animals* published by the US National Institutes of Health and was performed after securing approval by the Regierungspräsidium Freiburg.

Isolated working heart perfusion

Hearts were excised and placed into ice-cold Krebs-Henseleit Buffer (KHB) containing (in mmol/l) 128 NaCl, 5 KCl, 1 KH₂PO₄, 1.3 MgSO₄, 15 NaHCO₃, 2.5 CaCl₂ and 5 Glucose. Non-cardiac tissue was removed and the aorta was cannulated and secured to a 20-gauge plastic cannula. Following retrograde Langendorff perfusion (50 mmHg perfusion pressure) with KHB at 37°C, the left atrium was cannulated using an 18-gauge metal cannula, and perfusion was

switched to working mode with 15 mmHg preload and 50 mmHg afterload. After an initial equilibration period, hearts were perfused for 60 min with KHB containing 0.4 mmol/l palmitate bound to 3% BSA. Aortic pressure changes were measured using a pressure catheter placed inside the aortic cannula (Millar Micro-Tip, Millar Instruments, Houston, TX). Aortic developed pressure, cardiac output and cardiac power were quantified to evaluate contractile function. Myocardial oxygen consumption (MVO_2) was measured as difference of percent oxygen concentration in pre- and postcardial buffer samples using a fiber-optic oxygen sensor (Ocean Optics, Orlando, FL). Cardiac efficiency was calculated as ratio of hydraulic work to MVO_2 . Glucose oxidation and glycolytic flux were determined in the same perfusion using [$U-^{14}C$] glucose and [$5-^3H$] glucose (each specific activity 300 MBq/mol). Glucose oxidation was determined by the sum of trapped $^{14}CO_2$ in hyamine hydroxide and the presence of ^{14}C bicarbonate anion in the perfusate released from [$U-^{14}C$] glucose. Glycolytic flux was determined by measuring the amount of 3H_2O released from the metabolism of [$5-^3H$] glucose by separating H_2O from the perfusate using an anion exchange resin (200–400 mesh Dowex AG-1-X4) column technique. Palmitate oxidation was measured in separately perfused hearts by determining the amount of 3H_2O released from [$9,10-^3H$] palmitate (specific activity, 500 GBq/mol). For details, see [S1 Methods](#).

Myocardial triacylglycerol content

Triacylglycerol levels were quantified enzymatically in whole heart homogenates using the Serum Triglyceride Determination Kit (Sigma Aldrich, Taufkirchen, Germany).

Isoproterenol treatment

Mice were anesthetized with ketamin (100 mg/kg) and xylazin (40 mg/kg), and mini-osmotic pumps (250 μ l; Alzet, Cupertino, CA) were implanted subcutaneously in the intrascapular area. Pumps were filled under sterile conditions in accordance with manufacturer's instructions, containing 50 μ l 0.2% ascorbic acid and either body weight-adjusted amounts of isoproterenol (17mg/kg/day) or saline solution. Pumps had a mean flow rate of 0.25 μ l/h for 5 days before harvesting the hearts.

OXPHOS complex activities

Mitochondria were isolated by differential centrifugation as described before [18]. Protein concentration of mitochondrial suspensions was determined using the Micro BCA method (Pierce, Rockford, IL). Samples of fresh mitochondria were treated with 10 mg cholate/mg mitochondrial protein and diluted to a final concentration of 1 mg/ml with MSM/EDTA buffer (5 mmol/l mannitol, 220 mmol/l sucrose, 5 mmol/l MOPS, 2 mmol/l EDTA, pH 7.4) supplemented with 1 μ l/ml mammalian protease inhibitor cocktail (Sigma Aldrich, Taufkirchen, Germany). Complex I activity was measured based on a modified protocol by Janssen et al. [14]. 30 μ l of isolated mitochondria at a concentration of 0.1 g/l was added to 150 μ l incubation buffer (200 mmol/l KH_2PO_4 , 14,7 mmol/l BSA, 1.3 mmol/l 2,6-dichloroindophenol (DCIP), 10 mmol/l decylubichinon, 0.11 mmol/l antimycin A). After 3 minutes of incubation, 20 μ l 2.1 mmol/l NADH was added, and the reduction of DCIP was followed spectrophotometrically at 600 nm. After 60 s, 10 μ l of 0.15 mmol/l rotenone was added to inhibit complex I activity. Complex II activity was measured according to Krahenbuhl et al. [15] with modifications. 45 μ l of 0,5 g/l isolated mitochondria were added to 525 μ l incubation buffer (in mmol/l: KH_2PO_4 50, DCIP 0.05, antimycin A 0.005, duroquinone 0.5, EDTA 1; 1 g/l BSA) for 3 minutes. 60 μ l of 210 mmol/l succinate was added, and the reduction of DCIP was followed spectrophotometrically at 600 nm. Cytochrome c oxidase activity was

measured according to Wharton et al. [16]. Mitochondria (0.005 g/l) were measured in 175 μ l incubation buffer (50 mmol/l KH_2PO_4 , 0.04 mmol/l dodecyl- β -D-maltoside). 30 μ l of 0.28 mmol/l reduced cytochrome c was added and oxidized by complex IV, followed spectrophotometrically at 550 nm.

Mitochondrial respiration and ATP synthesis

Saponin-permeabilized cardiac fibers were prepared from freshly excised hearts as described previously [17,18]. Respiration rates of fibers were measured in a buffer (25°C) containing (in mmol/l) KCL 125, HEPES 20, Mg-Acetate 3, EGTA 0.4, BSA 2mg/ml, KH_2PO_4 5, DTT 0.3, glutamate 5, malate 2. Respiration was measured in the presence of substrate alone (V_0), after addition of 1 mmol/l ADP (V_{ADP}), and after addition of 1 μ g/ml oligomycin (V_{oligo}). To determine rates of ATP synthesis, separate experiments were performed with identical buffer conditions. 0.6 mmol/l ADP was added, and samples (10 μ l) were taken every 10 s for a total period of 1 min and added to 190 μ l DMSO. ATP content of ATP-containing DMSO samples was determined using a bioluminescence assay kit (Enliten Luciferase/Luciferin Reagent; Promega, Mannheim, Germany).

Immunoprecipitation

Whole hearts were homogenized in 500 μ l ice-cold lysis buffer (25 mmol/L Tris HCl, pH 7.4, 5 mmol/L MgCl_2 , 10% glycerol, 100 mmol/L KCl, 1% NP40, 0.3 mmol/L dithiothreitol, 5 μ l protease/phosphatase inhibitor cocktail, 5 mmol/L nicotinamide, 1 μ mol/L orthovanadate, 50 mmol/L sodium fluoride, 1 mmol/L sodium butyrate and 5 mmol/L sodium pyrophosphate), sonicated for 1 min using an Ultra-Turrax T10 basic (IKA Labortechnik, Staufen, Germany), and separated by centrifugation (10 000 x g for 30 min at 4°C). 500 μ g of protein were incubated with 50 μ l beads (1.5 mg) and 5 μ g anti-PGC-1 α antibody (Santa Cruz, Heidelberg, Germany), rotating overnight at 4°C. Beads were collected using a magnetic rack, washed with washing-buffer (Immunoprecipitation kit, Invitrogen, Carlsbad, CA), dissolved in loading buffer, and boiled. The immunoprecipitates were then separated by SDS-PAGE and immunoblotted using anti-PGC-1 α -antibody (1:200; Santa Cruz, Heidelberg, Germany) and subsequently with acetyl-lysine antibody (1:1.000; Cell Signaling, Boston, MA).

Western blot analysis

Proteins of whole heart homogenates or isolated mitochondria were separated by SDS-PAGE and transferred onto PVDF membranes (Bio-Rad Laboratories, Hercules, CA), probed with primary antibodies overnight at 4°C, washed with PBS, and probed with secondary antibodies for 1 h at room temperature. The following primary antibodies were used: Anti-AMPK 1:500 (# 2532, Cell Signaling, Boston, MA), Anti-phospho-AMPK Thr 172 1:500 (#2531, Cell signaling, Boston, MA), Anti-complex I NDUF8 subunit 1:2000 (#459210, Invitrogen, Carlsbad, CA), Anti-complex II Fp subunit 1:10000 (#MS204, Mitosciences, Eugene, OR), Anti-complex IV subunit IV 1:1000 (#MS407, Mitosciences, Eugene, OR), Anti-CTRP9 (#A00081-03-100, Aviscera Bioscience, Santa Clara, CA). Secondary antibodies: Anti-Mouse IgG Fab2 Alexa Fluor, Anti-Rabbit IgG (H+L) Fab2, Alexa Fluor 1:1000 (#4410, #4414, both Cell Signaling, Boston, MA). Detection and quantification of fluorescence bands was performed using the Odyssey imaging system (LI-COR Biosciences, Lincoln, NE). Loading control was performed using staining with Coomassie Blue R-250 (Bio-Rad, Hercules, CA).

Gene expression

Total RNA was isolated from hearts with TRIzol reagent (Invitrogen, Carlsbad, CA), purified with the RNEasy Kit (Qiagen, Hilden, Germany), and reverse transcribed using the SuperScript-III Reverse Transcriptase Kit (Invitrogen, Carlsbad, CA), as described before [17]. SYBR-green (Invitrogen, Carlsbad, CA) was used as probe, and amplification was monitored using the CF X96 Real-Time PCR system (Bio Rad, Munich, DE). Data were normalized by expressing them relative to the levels of the invariant transcript 16S ribosomal RNA and are presented as arbitrary units normalized to wildtype expression levels. Primer sequences and accession numbers are presented in [S1 Table](#).

SIRT1 activity

Freshly excised hearts were homogenized in buffer containing 250 mmol/L sucrose, 10 mmol/L Tris-HCl, and 1 mmol/L EDTA (adjusted to pH 7.4) using a Polytron homogenizer. The homogenate was frozen (liquid N₂) and thawed (37°C) three times, and SIRT1 activity was measured using the SIRT1 Drug Discovery Kit (Biomol, Hamburg, Germany). In brief, 0.5 mg/ml homogenate protein was incubated in 50 μ l Biomol assay buffer containing 0.05 mmol/L *Fluor de Lys* SIRT1 substrate and 5 μ mol/L NAD⁺ \pm 2.5 mmol/L suramin, incubated at 37°C for 45 min, and fluorophore generation equivalent to deacetylated SIRT1 substrate levels was measured 15 min following addition of 50 μ l 1mmol/L nicotinamide and Developer II solution in a fluorescence plate reader (Excitation: 360nm, Emission: 460nm).

Electron microscopy

Left ventricular samples were fixed in 2.5% glutaraldehyde and 1% paraformaldehyde, post-fixed in 2% osmium, embedded in resin, and sectioned (thickness 80–100 nm). Mitochondrial morphology was assessed at x 2,000 and x 40,000 magnifications. Mitochondrial volume density was analyzed by stereology in a blinded fashion using the pointcounting method [17,19].

Statistical analysis

Data are presented as means \pm SE. When comparing two groups, significance was determined using a Student's t test. Data generated following isoproterenol treatment were analyzed using a 2-way analysis of variance (2-way ANOVA) followed by a Bonferroni post-hoc test. For all analyses, GraphPad Prism software was used (GraphPad Software, Inc., La Jolla, CA), and significant difference was accepted when $p < 0.05$.

Results

Preserved mitochondrial and contractile function in hearts of ADQ^{-/-} mice

Male animals were investigated at 8 weeks of age. Serum adiponectin levels were 24 μ g/ml in WT mice, which is consistent with other reports [1,20]. As expected, serum adiponectin was literally not detectable in ADQ^{-/-} mice ([S1 Fig](#)). In glucose tolerance tests, ADQ^{-/-} mice showed no difference in glucose clearance compared to WT mice ([S1 Fig](#)). Serum levels of free fatty acids and triglycerides were significantly lower in ADQ^{-/-} mice ([S1 Fig](#)). While heart weights and body weights were mildly increased in ADQ^{-/-} mice, heart weight-to-body weight ratios were not different compared to WT mice ([S2 Table](#)).

ADQ^{-/-} and WT mice were perfused in the isolated working heart mode. Cardiac power, aortic developed pressure and cardiac output were all unchanged between groups ([Fig 1](#)). Cardiac power was also unchanged between ADQ^{-/-} and WT mice when analyzing contractile function separately in perfusions measuring fatty acid oxidation or glucose oxidation, although

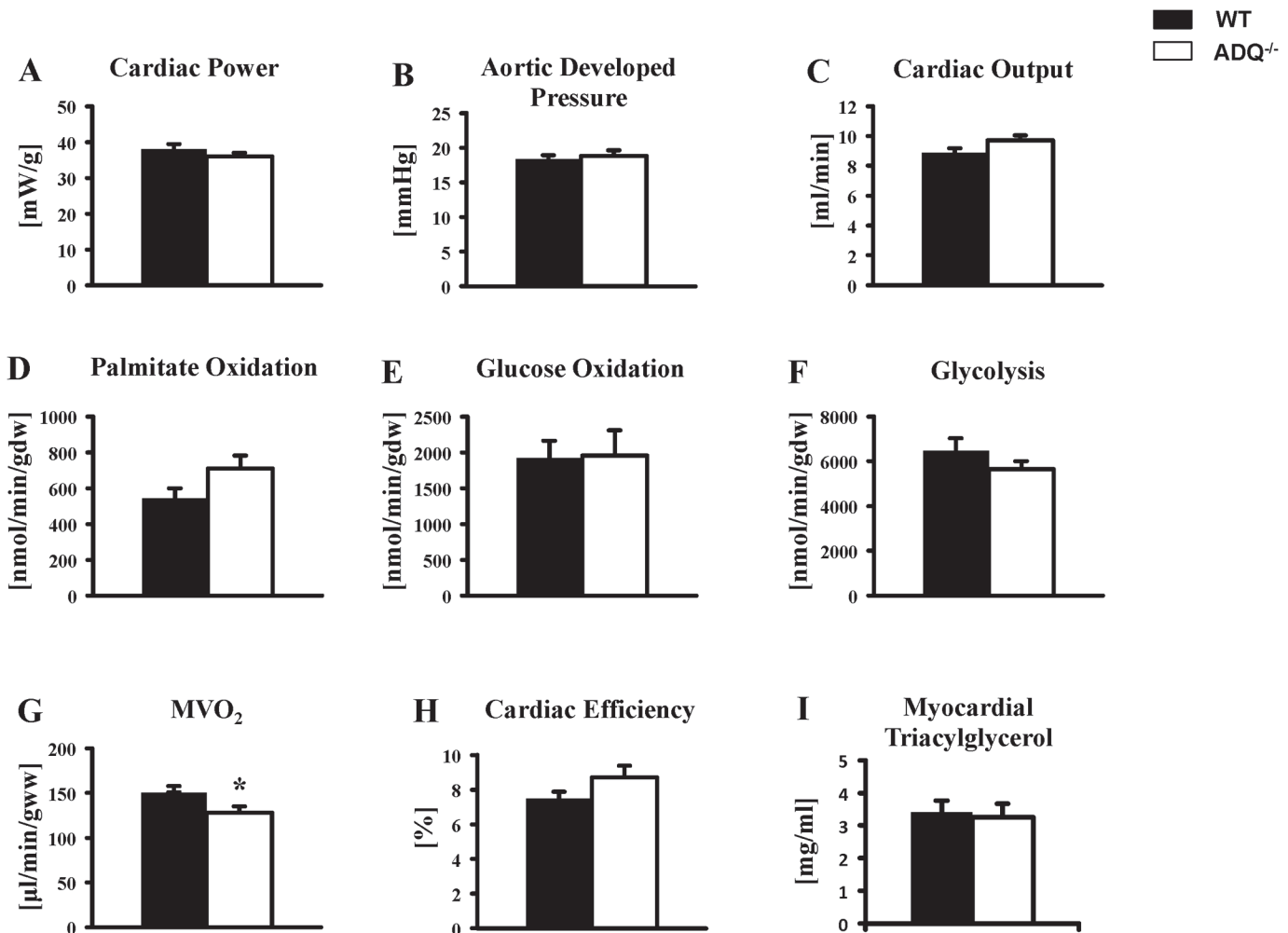


Fig 1. Preserved contractile function in ADQ^{-/-} hearts. Cardiac power (A), aortic developed pressure (B), cardiac output (C), palmitate oxidation (D), glucose oxidation (E), glycolysis (F), MVO₂ (G), and cardiac efficiency (H) in isolated working hearts of ADQ^{-/-} and WT mice at 8 weeks of age; n = 4–6 for substrate oxidation, n = 10 for contractile parameters. (I) Myocardial triacylglycerol levels in ADQ^{-/-} and WT mice at 8 weeks of age; n = 4–5. * p < 0.05 vs. WT.

doi:10.1371/journal.pone.0119416.g001

cardiac power was higher both in WT and ADQ^{-/-} mice in the glucose oxidation group compared to the fatty acid oxidation group (S2 Fig.). Rates of palmitate oxidation, glucose oxidation and glycolysis were also not different between groups (Fig. 1). When relating substrate oxidation rates to cardiac work, palmitate and glucose oxidation rates were also not different between groups, although glycolysis rates were now reduced in ADQ^{-/-} mice compared to WT mice (S3 Fig.). A mild but significant decrease in MVO₂ in ADQ^{-/-} mice did not result in a relevant increase in cardiac efficiency (Fig. 1). Myocardial triacylglycerol levels were unchanged between groups (Fig. 1). Thus, cardiac contractile function and energy substrate utilization rates were mainly unaffected in the absence of adiponectin.

Mitochondrial function was evaluated in saponin-permeabilized cardiac fibers. V₀, V_{ADP} and V_{Oligo} were unchanged between ADQ^{-/-} and WT mice, using palmitoyl-carnitine, glutamate or pyruvate as substrate (Fig. 2). Similarly, rates of ATP synthesis were unchanged between groups with any substrate, resulting in unchanged ATP/O ratios (Fig. 2). In addition, we determined enzymatic activities of OXPHOS complexes. While complex IV showed a significant decrease in enzymatic activity, activities of complexes I and II were unchanged (Fig. 3).

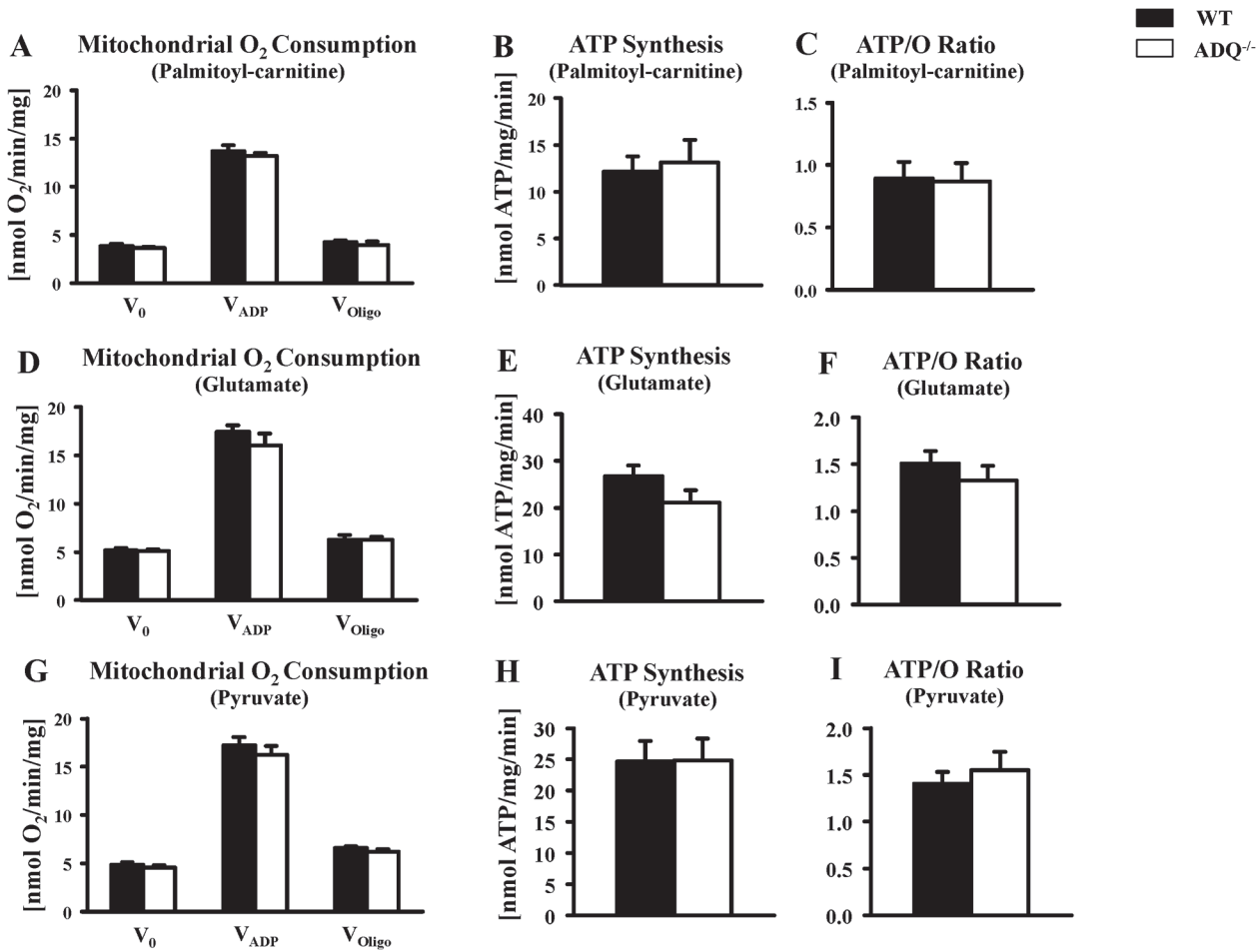


Fig 2. Preserved mitochondrial function in ADQ^{-/-} hearts. Mitochondrial O₂ consumption rates, ATP synthesis rates, and ATP/O ratios in saponin-permeabilized cardiac fibers of ADQ^{-/-} and WT mice, using palmitoyl-carnitine (A-C), glutamate (D-F), or pyruvate (G-I) as substrate; n = 6.

doi:10.1371/journal.pone.0119416.g002

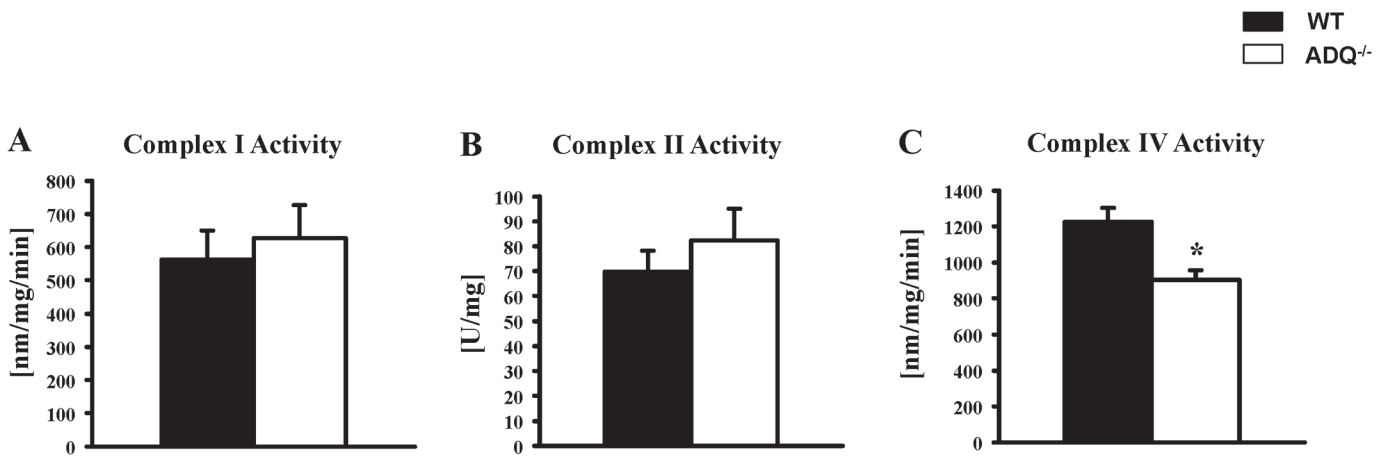


Fig 3. Preserved mitochondrial OXPHOS complex activities in ADQ^{-/-} hearts. Enzymatic activity of complex I subunit NDUFB8 (A), complex II subunit 30kDa (B), and complex IV subunit II (C) in isolated mitochondria of ADQ^{-/-} and WT hearts; n = 5–6. * p<0.05 vs. WT.

doi:10.1371/journal.pone.0119416.g003

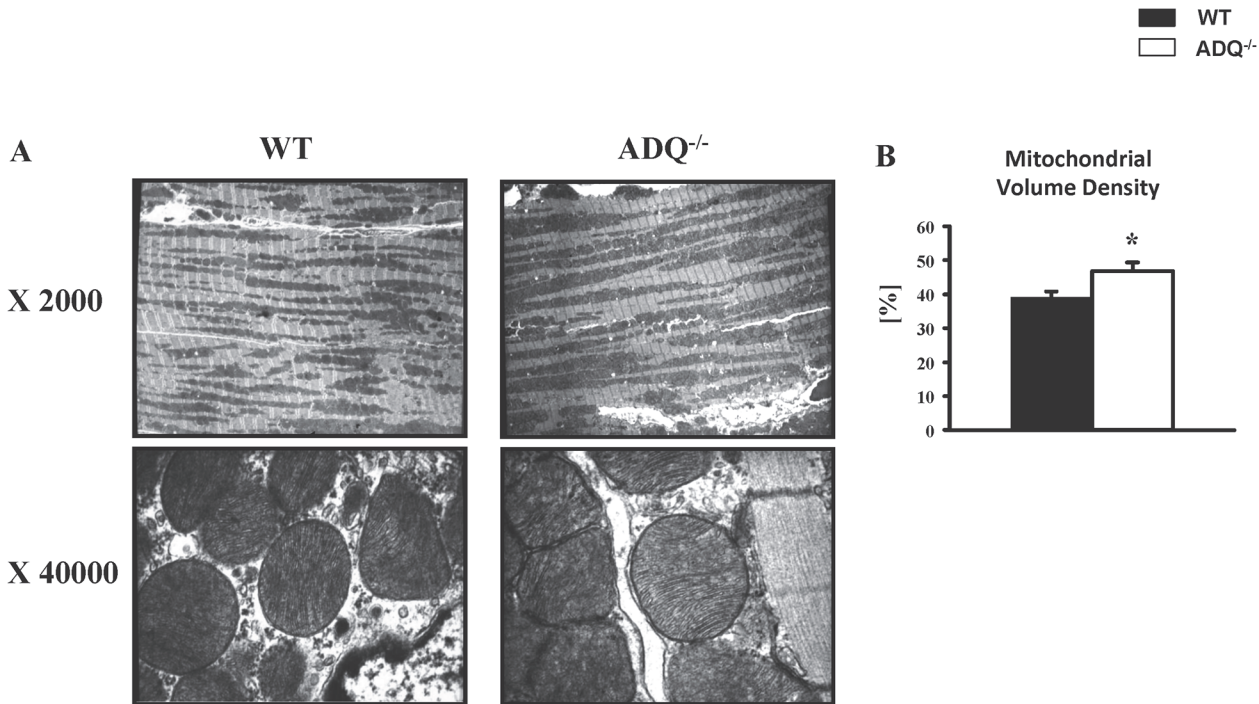


Fig 4. Preserved mitochondrial morphology in ADQ^{-/-} hearts. Representative electron microscopy images at magnification x 2000 or x 40000 (A), and stereologic quantification of mitochondrial volume density (B) of 8 week-old ADQ^{-/-} and WT hearts; n = 4. * p<0.05 vs. WT.

doi:10.1371/journal.pone.0119416.g004

Mitochondrial ultrastructure was analyzed using electron microscopy. Mitochondria were embedded in regular fashion between myofibers without disarrays, and cristae density and membrane morphology appeared identical in ADQ^{-/-} and WT mice (Fig. 4). Mitochondrial volume density was even slightly increased in ADQ^{-/-} mice (Fig. 4). Taken together, mitochondrial function was preserved in hearts of ADQ^{-/-} mice.

In skeletal muscle, lack of adiponectin impairs AMPK phosphorylation and SIRT1 activity and thereby signaling via PGC-1 α , resulting in decreased expression of OXPHOS genes [6]. In ADQ^{-/-} hearts, AMPK phosphorylation was not decreased but even increased compared to WT hearts (Fig. 5). Both SIRT1 activity and lysine acetylation of PGC-1 α were not different between groups (Fig. 5). While mRNA expression of two OXPHOS subunits and of medium chain acyl-CoA dehydrogenase (Mcad) was reduced in ADQ^{-/-} hearts, mRNA expression of six other OXPHOS subunits was unchanged (Fig. 5). On the protein level, mitochondrial content of OXPHOS complexes I (subunit NDUF8), II (subunit 30kDa) and IV (subunit II) was not reduced or even increased in ADQ^{-/-} mice (Fig. 5). In addition, mRNA expression of transcription factors and cofactors involved in mitochondrial biogenesis was maintained, including PGC-1 α , and ERR α mRNA expression was even increased in ADQ^{-/-} mice (Fig. 5). Thus, lack of adiponectin did not impair mitochondrial biogenic signaling in the heart.

Preserved mitochondrial and contractile function in hearts of ADQ^{-/-} mice in response to prolonged isoproterenol stimulation

To investigate the response to a prolonged increase in energy demand, mice were subjected to prolonged beta-adrenergic stimulation by continuous subcutaneous infusion of isoproterenol for 5 days using mini-osmotic pumps. Isoproterenol infusion resulted in increased heart weight-to-body weight ratios both in WT and ADQ^{-/-} mice compared to saline-treated mice, but no

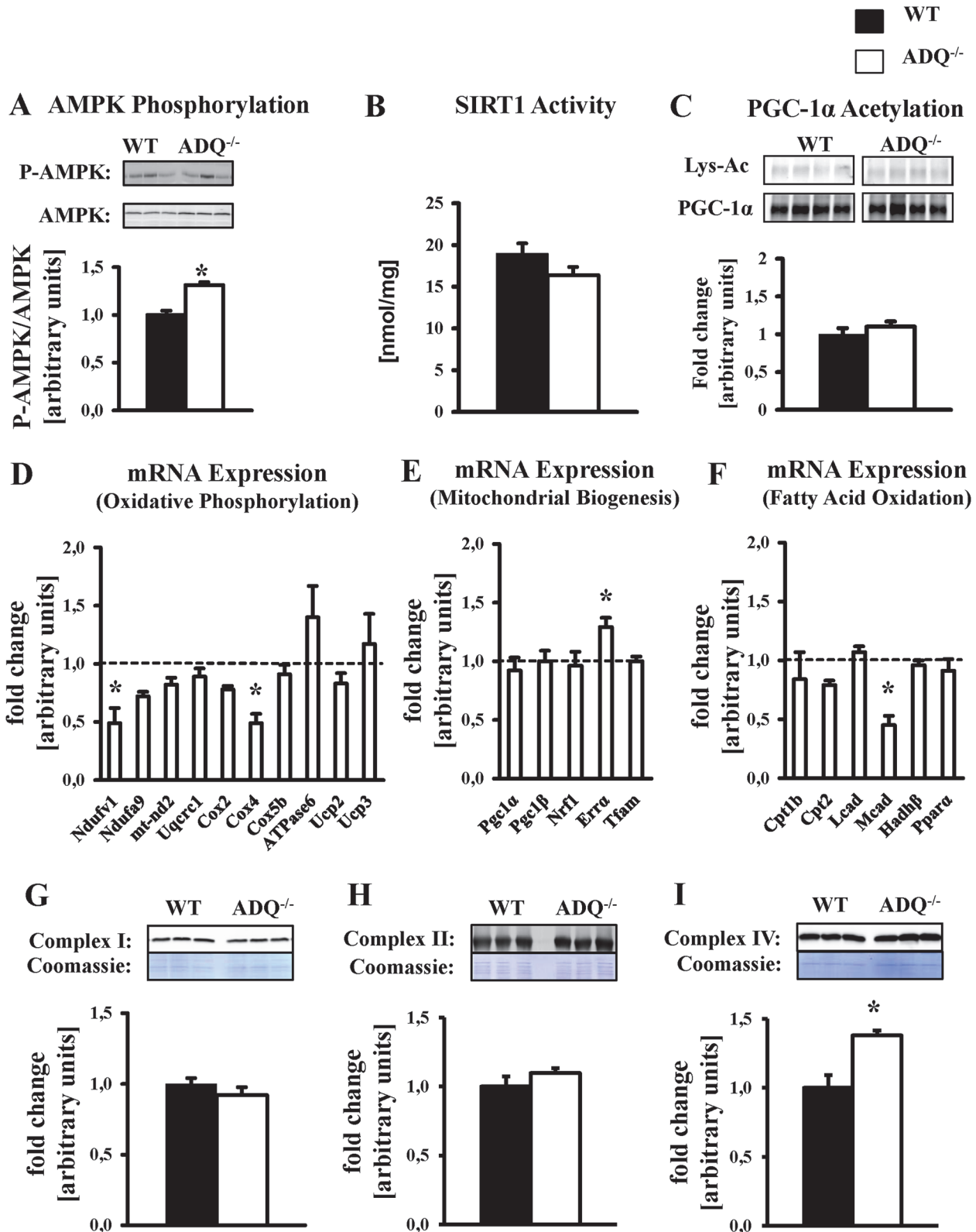


Fig 5. Preserved OXPHOS protein levels and mitochondrial biogenic signaling in ADQ^{-/-} hearts. AMPK phosphorylation (A), SIRT1 activity (B), lysine acetylation (Lys-Ac) of PGC-1α (C), mRNA expression of OXPHOS subunits (D), mRNA expression of mitochondrial biogenesis signaling molecules (E), mRNA expression of fatty acid oxidation genes and PPARα (F), and mitochondrial protein levels of OXPHOS complexes I (NDUFB8 subunit; G), II (Fp

subunit; H), and IV (subunit IV; I) in hearts of ADQ^{-/-} and WT mice at 8 weeks of age; n = 4–5. Myocardial mRNA expression is expressed relative to WT expression which was set to 1 (indicated by the dotted line). * p<0.05 vs. WT.

doi:10.1371/journal.pone.0119416.g005

difference was observed between isoproterenol-treated WT and ADQ^{-/-} mice (S3 Table). While aortic developed pressure remained unchanged among groups in isolated working hearts following isoproterenol infusion, cardiac output and cardiac power were reduced in isoproterenol-treated mice compared to saline-treated mice, likely due to a decrease in heart rate in the isoproterenol-treated groups (Fig. 6). Importantly, no differences in contractile function were observed between ADQ^{-/-} and WT mice following isoproterenol treatment. MVO₂ showed an additional decrease in ADQ^{-/-} mice compared to WT mice following isoproterenol treatment, which however did not result in a significant increase in cardiac efficiency in isoproterenol-treated ADQ^{-/-} mice (Fig. 6). Thus, the contractile response following prolonged beta-adrenergic stimulation was similar between ADQ^{-/-} and WT mice.

Mitochondrial function was investigated following prolonged isoproterenol stimulation. In saponin-permeabilized cardiac fibers, V_{ADP} was increased in ADQ^{-/-} and WT mice following

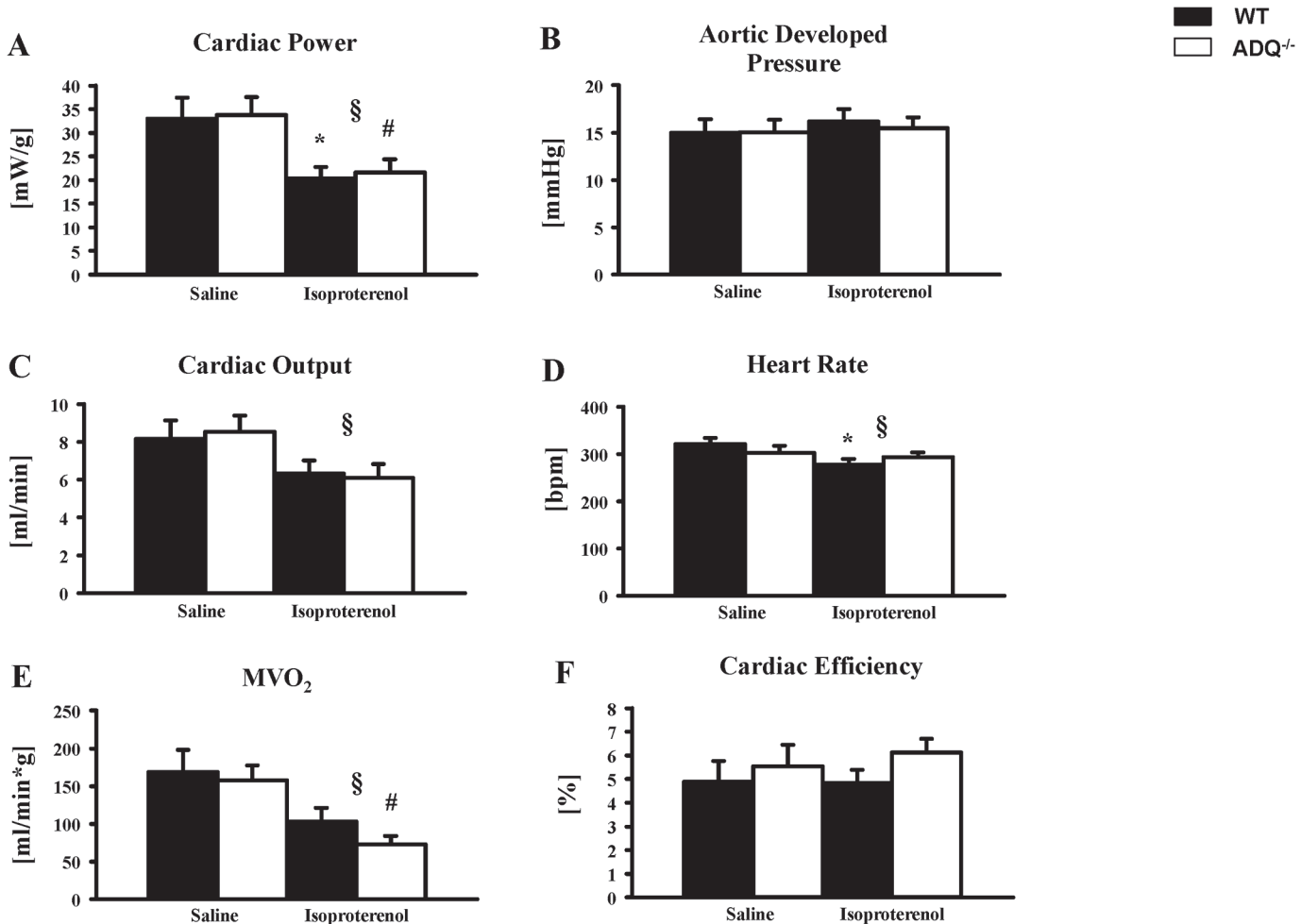


Fig 6. Similar contractile response of ADQ^{-/-} hearts to isoproterenol stimulation. Heart weight-to-tibia length ratios (A), and aortic developed pressure (B), cardiac output (C), cardiac power (D), MVO₂ (E), and cardiac efficiency (F) in isolated working hearts of ADQ^{-/-} and WT mice subjected to 5 days of continuous subcutaneous isoproterenol infusion; n = 4. 2-way ANOVA: § effect of isoproterenol, * p<0.05 vs. WT saline, # p<0.05 vs. ADQ^{-/-} saline.

doi:10.1371/journal.pone.0119416.g006

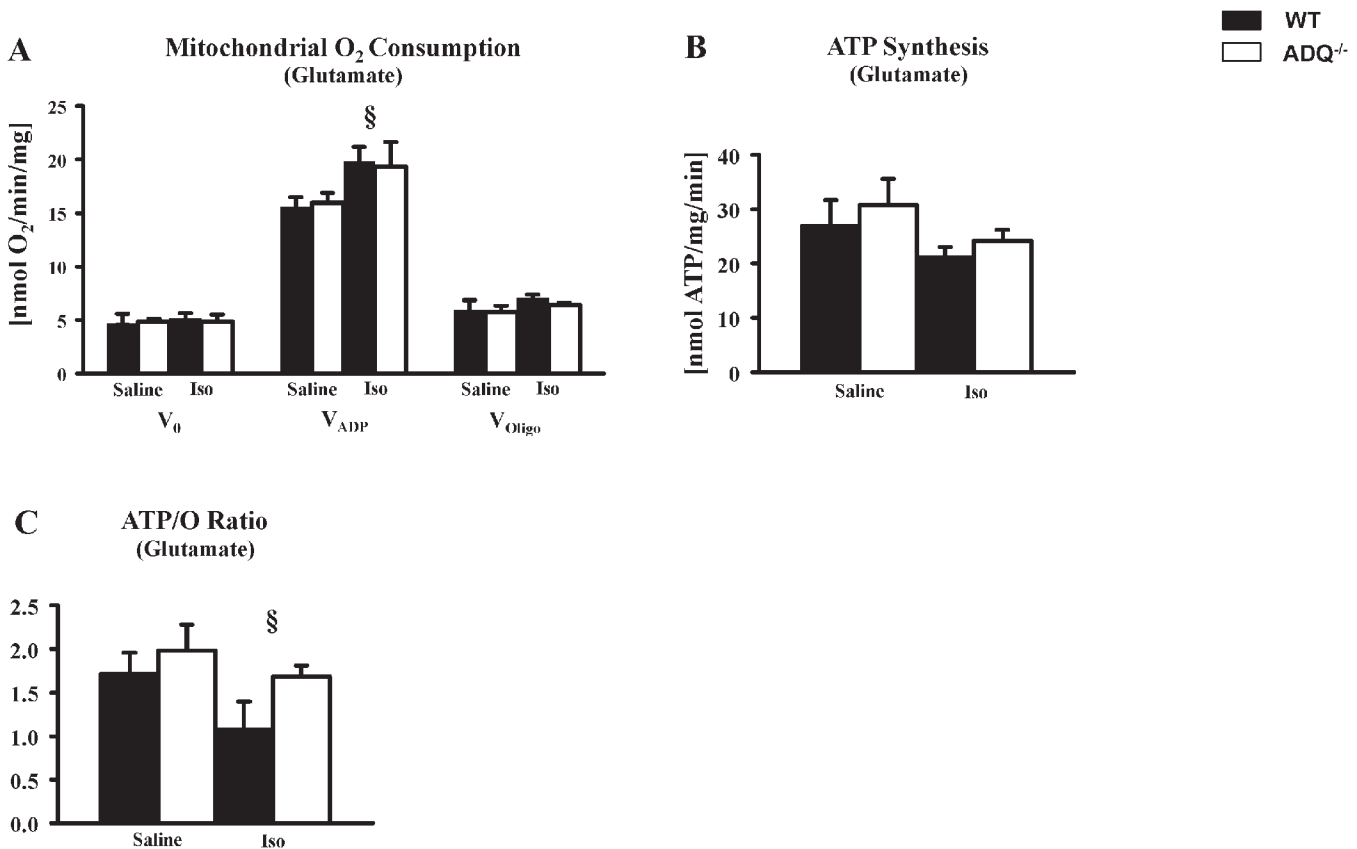


Fig 7. Preserved mitochondrial function in ADQ^{-/-} hearts following isoproterenol treatment. Mitochondrial O₂ consumption rates (A), ATP synthesis rates (B), and ATP/O ratios (C) in saponin-permeabilized cardiac fibers of ADQ^{-/-} and WT mice using glutamate as substrate; n = 4. 2-way ANOVA: § effect of isoproterenol.

doi:10.1371/journal.pone.0119416.g007

isoproterenol treatment compared to saline-treated mice (Fig. 7). However, V_{ADP} was not different between ADQ^{-/-} and WT mice. Similarly, no changes in ATP synthesis were observed between genotypes following isoproterenol treatment (Fig. 7). ATP/O ratios were decreased following isoproterenol treatment compared to saline-treated mice, whereas no differences were observed between ADQ^{-/-} and WT mice following isoproterenol or saline treatment.

Increased serum protein levels of CTRP9 in ADQ^{-/-} mice

C1q/TNF-related proteins (CTRPs) are recently discovered adiponectin paralogs which bind to adiponectin receptors and may mimic adiponectin effects on cellular physiology [21]. In particular, CTRP9 has been shown to increase AMPK activity and mitochondrial content in skeletal muscle, and is able to signal via adiponectin receptor 1 [27,28]. CTRPs circulate in the bloodstream and/or are expressed in cells in a tissue-specific manner. Of the 15 CTRPs identified thus far, we were able to detect the mRNA expression of 8 CTRPs in myocardial tissue. While myocardial mRNA expression of CTRP3 and CTRP4 was reduced in ADQ^{-/-} mice, the expression of CTRP1, 5, 6, 7, 9 and 13 was not different compared to WT mice (Fig. 8). In contrast, serum protein levels of CTRP9 were increased in ADQ^{-/-} mice (Fig. 8), suggesting that increased CTRP9 signaling via adiponectin receptors may compensate for the lack of adiponectin action in ADQ^{-/-} mice.

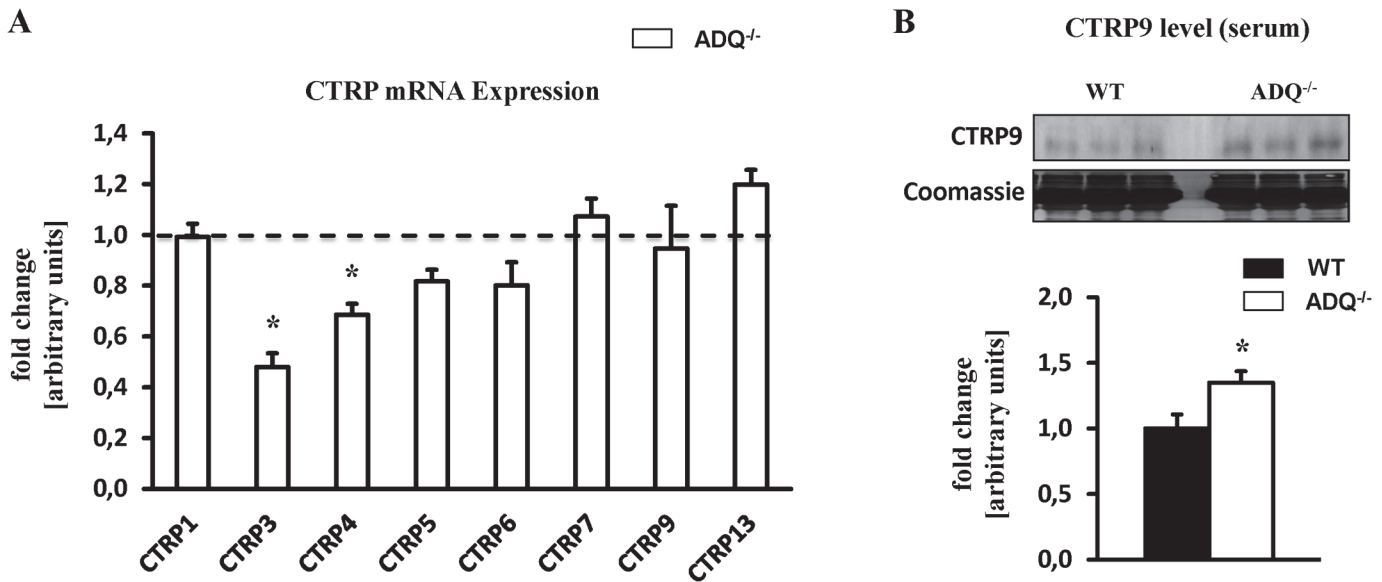


Fig 8. Myocardial expression of CTRPs. (A) Myocardial mRNA expression of CTRP1, 3, 4, 5, 6, 7, 9 and 13 in ADQ^{-/-} mice at 8 weeks of age, relative to WT expression which was set to 1 (indicated by the dotted line); n = 8. (B) Serum CTRP9 protein levels in ADQ^{-/-} and WT mice at 8 weeks of age; n = 5. * p < 0.05 vs. WT.

doi:10.1371/journal.pone.0119416.g008

Discussion

In the current study, we investigated mitochondrial energetics and cardiac function in mice lacking adiponectin. Mitochondrial respiratory capacity, ATP synthesis, activities of OXPHOS complexes I and II, and mitochondrial biogenic signaling were unaffected by lack of adiponectin. Similarly, myocardial contractile function was unaffected, even in response to prolonged beta-adrenergic stimulation with isoproterenol. Thus, mitochondrial and contractile function are preserved in hearts of mice lacking adiponectin, suggesting that adiponectin may be expendable in the regulation of mitochondrial energetics and contractile function in the heart under non-pathologic conditions.

We show here that mitochondrial respiratory capacity and ATP synthesis were not impaired in saponin-permeabilized cardiac fibers of AdQ^{-/-} mice. Similarly, activity of OXPHOS complexes I and II was not different between groups, and signaling via the AMPK-PGC-1 α axis appeared unaffected by adiponectin deficiency. Finally, rates of oxidative substrate utilization in isolated working hearts were not impaired in AdQ^{-/-} mice. These data are in line with O'Shea et al. who reported of unaffected citrate synthase activity in adiponectin knockout mice [22,23]. In contrast, Yan et al. reported a decrease in AMPK phosphorylation, an increase in PGC-1 α acetylation, and a mild decrease of the enzymatic activity of OXPHOS complexes I, III and V in ADQ^{-/-} mice, concluding that impaired mitochondrial biogenic signaling may impair mitochondrial function in mice lacking adiponectin [24]. Unfortunately, mitochondrial respiratory capacity, which includes the activity of all OXPHOS complexes and is considered as an overall measure of mitochondrial function, was not reported, thereby limiting conclusions on overall mitochondrial function. In addition, no data on gene or protein expression of OXPHOS complex subunits was presented, limiting the conclusion of impaired mitochondrial biogenesis as a mechanism contributing to impaired OXPHOS complex activity in mice lacking adiponectin. In the current study, we found no convincing evidence of impairment in AMPK-PGC-1 α signaling, mitochondrial respiration, ATP synthesis, and gene and protein expression of

OXPPOS subunits. Thus, we would argue that, in this model of adiponectin deficiency, adiponectin may not be essential to maintain mitochondrial function in the heart.

Cardiac function in isolated working hearts was not impaired in $AdQ^{-/-}$ mice under non-stressed conditions. This finding is in line with several other reports showing no impairment of cardiac function in adiponectin knockout mice using echocardiography [13,23,25], suggesting that adiponectin deficiency may not be required to maintain physiological cardiac function under non-stressed conditions. Following prolonged beta-adrenergic stimulation with isoproterenol for 5 days, both contractile and mitochondrial function were not differentially affected in $ADQ^{-/-}$ mice compared to WT mice. Thus, even when increasing energy demand for prolonged time periods, adiponectin deficiency does not seem to predispose for myocardial energy depletion. When extrapolating these results, one may argue that impaired energetics may also not contribute to exaggerated hypertrophy following pressure overload, although the adaptive mechanisms in response to increased energy demand due to aortic constriction are quite different compared to increased beta-adrenergic stimulation as occurs in the isoproterenol model. Ultimately, myocardial energetics need to be investigated in adiponectin-deficient mice following aortic constriction to evaluate a contribution of impaired energetics to exaggerated hypertrophy.

When integrating both the data on mitochondrial function from Yan et al. [24] and our study, one needs to conclude that adiponectin deficiency in the mouse model generated by Chan and colleagues [26] only mildly impairs myocardial mitochondrial function at the most. It can however not be ruled out that other members of the C1q/TNF-related protein (CTRP) family with high amino acid sequence homology to adiponectin may compensate for the lack of adiponectin action by mimicking adiponectin action and signaling. CTRPs circulate in the bloodstream and/or are expressed in cells in a tissue-specific manner. First, we investigated myocardial mRNA expression of all detectable CTRPs, which revealed decreased mRNA expression for CTRP3 and CTRP4, and unchanged expression for the remaining detectable CTRPs in $ADQ^{-/-}$ mice. CTRP3 replenishment following myocardial infarction has been shown to improve survival rates, to restore cardiac function, to attenuate cardiomyocyte apoptosis, to reduce fibrosis, and to increase revascularization, thus suggesting that reduced myocardial CTRP3 expression rather does not result in compensatory effects in the absence of adiponectin [29]. The functional effects of CTRP4 are largely unknown, particularly in the heart. In contrast, when looking at circulating CTRPs, we found increased serum protein levels of CTRP9 in $ADQ^{-/-}$ mice (Fig. 8B). Since overexpression of CTRP9, the closest paralog of adiponectin, has been shown to increase AMPK activity and mitochondrial content in skeletal muscle, and since CTRP9 is able to signal via adiponectin receptor 1 [27,28], increased CTRP9 signaling via adiponectin receptor 1 may compensate for the lack of adiponectin action in $ADQ^{-/-}$ mice. We did not investigate serum levels of other CTRPs or the expression of CTRPs in extramyocardial tissues in $ADQ^{-/-}$ mice, which needs to be addressed in future studies in this animal model. Finally, studies using mice with deficiency of adiponectin receptors may allow a more differentiated view on the role of adiponectin signaling in myocardial energetics and may circumvent potential confounding effects by CTRPs.

It remains to be mentioned that adiponectin deficiency has been shown to impair mitochondrial function and biogenesis in extracardiac tissues such as skeletal muscle. Civitarese and colleagues showed that mitochondrial DNA copy number, cytochrome c oxidase activity and citrate synthase activity were impaired in skeletal muscle of adiponectin-deficient mice generated by Philipp Scherer's group [5, 30]. In addition, Iwabu and colleagues demonstrated that lack of adiponectin receptor 1 in skeletal muscle also impairs mitochondrial DNA content, PGC-1 α signaling and mitochondrial F_0F_1 -ATPase activity [6]. It remains to be elucidated whether tissue-specific differences in adiponectin action and/or compensatory mechanisms in

our animal model may be responsible for the different effects of adiponectin deficiency on myocardial mitochondrial biology. Compensatory mechanisms may include increased CTRP9 action on myocardial adiponectin receptors (Fig. 8B), or adaptive posttranslational mechanisms as suggested by increased mitochondrial Cox2 protein levels despite unchanged Cox2 mRNA expression (Fig. 5D, I).

In conclusion, our data suggest that, at least in the model used in this study, adiponectin is not required to maintain mitochondrial energetics and contractile function in the heart under non-pathological conditions. A possible compensating effect due to increased CTRP9 action, which may mimic cellular adiponectin effects, cannot be ruled out. Analysis of adiponectin receptor signaling and downstream effects in the myocardium will help to further elucidate the relevance of myocardial adiponectin action for cardiac energetics and for myocardial adaptations in response to pathologic stressors.

Supporting Information

S1 Fig. Glucose tolerance, serum adiponectin and serum metabolite levels. Serum adiponectin levels (A), glucose tolerance test (B), and serum levels of free fatty acids (C) and triglycerides (D) in ADQ^{-/-} and WT mice at 8 weeks of age; n = 5–6. * p<0.05 vs. WT. (TIFF)

S2 Fig. Cardiac power in different working heart perfusion groups. Cardiac power calculated separately for ADQ^{-/-} and WT mice used to measure palmitate oxidation or used to measure glucose oxidation; n = 4–6. * p<0.05. (TIFF)

S3 Fig. Substrate oxidation normalized to cardiac work. Rates of palmitate oxidation (A), glycolysis (B) and glucose oxidation (C) normalized to cardiac work in ADQ^{-/-} and WT mice. (TIFF)

S1 Methods. Detailed description of serum metabolite measurements, glucose tolerance tests and isolated working heart experiments. (DOCX)

S1 Table. Sequences of forward and reverse primers used for RT-PCR. Abbreviations: ATPase6, ATP synthase F0 subunit 6; Cox II, cytochrome c oxidase subunit II; Cox IV, cytochrome c oxidase subunit IV; Cox Vb, cytochrome c oxidase subunit Vb; Cpt1b, carnitine palmitoyltransferase 1b; Cpt2, carnitine palmitoyltransferase 2; CTRP, C1q/TNF-related protein; Errα, estrogen related receptor alpha; Hadhβ, hydroxyacyl-CoA dehydrogenase, β subunit; Lcad, long chain acyl-CoA dehydrogenase; mt-Nd2, NADH dehydrogenase 2, mitochondrial; Mcad, medium chain acyl-CoA dehydrogenase; Ndufv1, NADH dehydrogenase [ubiquinone] flavoprotein 1; Ndufa9, NADH dehydrogenase [ubiquinone] 1 alpha subcomplex subunit 9; Uqcrc1, ubiquinol cytochrome c reductase core protein 1; Nrf1, nuclear respiratory factor 1; Pgc-1α, peroxisome proliferator-activated receptor gamma coactivator 1 alpha; Pgc-1β, peroxisome proliferator-activated receptor gamma coactivator 1 beta; PPARα, peroxisome proliferator-activated receptor α; Tfam, mitochondrial transcription factor A; Ucp2, uncoupling protein 2; Ucp3, uncoupling protein 3. (DOCX)

S2 Table. Similar heart weight-to-body weight ratio in ADQ^{-/-} mice. Heart weights related to body weight in ADQ^{-/-} and WT mice at 8 weeks of age; n = 10. * p<0.05 vs. WT. (DOCX)

S3 Table. Effect of isoproterenol treatment on heart weight-to-body weight ratio in WT and ADQ^{-/-} mice. Heart weights, body weights and heart weight-to-body weight (HW-BW) ratios in ADQ^{-/-} and WT mice following isoproterenol or saline treatment; n = 7. 2-way ANOVA: § effect of isoproterenol, § effect of genotype. * p<0.05 vs. WT saline, # p<0.05 vs. ADQ^{-/-} saline. (DOCX)

Acknowledgments

We would like to thank Judith Asal for technical assistance.

Author Contributions

Conceived and designed the experiments: HB TD CB MH MO. Performed the experiments: MB NH MCC KP CK. Analyzed the data: MB NH MCC KP CK HB MO. Wrote the paper: HB CB MH TD.

References

1. Maeda K, Okubo K, Shimomura I, Funahashi T, Matsuzawa Y, Matsubara K. cDNA cloning and expression of a novel adipose specific collagen-like factor, apM1 (AdiPose Most abundant Gene transcript 1). *Biochem Biophys Res Commun*. 1996; 221: 286–289. PMID: [8619847](#)
2. Fruebis J, Tsao TS, Javorschi S, Ebbets-Reed D, Erickson MR, Yen FT, et al. Proteolytic cleavage product of 30-kDa adipocyte complement-related protein increases fatty acid oxidation in muscle and causes weight loss in mice. *Proc Natl Acad Sci U S A*. 2001; 98: 2005–2010. PMID: [11172066](#)
3. Yamauchi T, Kamon J, Ito Y, Tsuchida A, Yokomizo T, Kita S, et al. Cloning of adiponectin receptors that mediate antidiabetic metabolic effects. *Nature*. 2003; 423: 762–769. PMID: [12802337](#)
4. Tomas E, Tsao TS, Saha AK, Murrey HE, Zhang Cc, Itani SI, et al. Enhanced muscle fat oxidation and glucose transport by ACRP30 globular domain: acetyl-CoA carboxylase inhibition and AMP-activated protein kinase activation. *Proc Natl Acad Sci U S A*. 2002; 99: 16309–16313. PMID: [12456889](#)
5. Civitarese AE, Ukropcova B, Carling S, Hulver M, DeFronzo RA, Mandarino L, et al. Role of adiponectin in human skeletal muscle bioenergetics. *Cell Metab*. 2006; 4: 75–87. PMID: [16814734](#)
6. Iwabu M, Yamauchi T, Okada-Iwabu M, Sato K, Nakagawa T, Funata M, et al. Adiponectin and AdipoR1 regulate PGC-1 α and mitochondria by Ca²⁺ and AMPK/SIRT1. *Nature*. 2010; 464: 1313–1319. doi: [10.1038/nature08991](#) PMID: [20357764](#)
7. Boudina S, Sena S, O'Neill BT, Tathireddy P, Young ME, Abel ED. Reduced mitochondrial oxidative capacity and increased mitochondrial uncoupling impair myocardial energetics in obesity. *Circulation*. 2005; 112: 2686–2695. PMID: [16246967](#)
8. Bugger H, Abel ED. Mitochondria in the diabetic heart. *Cardiovasc Res*. 2010; 88: 229–240. doi: [10.1093/cvr/cvq239](#) PMID: [20639213](#)
9. Lesnefsky EJ, Moghaddas S, Tandler B, Kerner J, Hoppel CL. Mitochondrial dysfunction in cardiac disease: ischemia-reperfusion, aging, and heart failure. *J Mol Cell Cardiol*. 2001; 33: 1065–1089. PMID: [11444914](#)
10. Ouchi N, Kihara S, Arita Y, Maeda K, Kuriyama H, Okamoto Y, et al. Novel modulator for endothelial adhesion molecules: adipocyte-derived plasma protein adiponectin. *Circulation*. 1999; 100: 2473–2476. PMID: [10604883](#)
11. Shibata R, Sato K, Pimentel DR, Takemura Y, Kihara S, Ohashi K, et al. Adiponectin protects against myocardial ischemia-reperfusion injury through AMPK- and COX-2-dependent mechanisms. *Nat Med*. 2005; 11: 1096–1103. PMID: [16155579](#)
12. Hong SJ, Park CG, Seo HS, Oh DJ, Ro YM. Associations among plasma adiponectin, hypertension, left ventricular diastolic function and left ventricular mass index. *Blood Press*. 2004; 13: 236–242. PMID: [15581338](#)
13. Shibata R, Ouchi N, Ito M, Kihara S, Shiojima I, Pimentel DR, et al. Adiponectin-mediated modulation of hypertrophic signals in the heart. *Nat Med*. 2004; 10: 1384–1389. PMID: [15558058](#)
14. Janssen AJ, Trijbels FJ, Sengers RC, Smeitink JA, van den Heuvel LP, Wintjes LT, et al. Spectrophotometric assay for complex I of the respiratory chain in tissue samples and cultured fibroblasts. *Clin Chem*. 2007; 53: 729–734. PMID: [17332151](#)

15. Krahenbuhl S, Chang M, Brass EP, Hoppel CL. Decreased activities of ubiquinol:ferricytochrome c oxidoreductase (complex III) and ferrocycytochrome c: oxygen oxidoreductase (complex IV) in liver mitochondria from rats with hydroxycobalamin[c-lactam]-induced methylmalonic aciduria. *J Biol Chem.* 1991; 266: 20998–21003. PMID: [1657942](#)
16. Tzagoloff A, Wharton DC. Studies on the Electron Transfer System. Lxii. The Reaction of Cytochrome Oxidase with Carbon Monoxide. *J Biol Chem.* 1965; 240: 2628–2633. PMID: [14304878](#)
17. Bugger H, Boudina S, Hu XX, Tuinei J, Zaha VG, Theobald HA, et al. Type 1 diabetic akita mouse hearts are insulin sensitive but manifest structurally abnormal mitochondria that remain coupled despite increased uncoupling protein 3. *Diabetes.* 2008; 57: 2924–2932. doi: [10.2337/db08-0079](#) PMID: [18678617](#)
18. Bugger H, Chen D, Riehle C, Soto J, Theobald HA, Hu XX, et al. Tissue-specific remodeling of the mitochondrial proteome in type 1 diabetic akita mice. *Diabetes.* 2009; 58: 1986–1997. doi: [10.2337/db09-0259](#) PMID: [19542201](#)
19. Weibel ER. Steriological principles for morphometry in electron microscopic cytology. *Int Rev Cytol.* 1979; 26: 235–302.
20. Arita Y, Kihara S, Ouchi N, Takahashi M, Maeda K, Miyagawa J, et al. Paradoxical decrease of an adipose-specific protein, adiponectin, in obesity. *Biochem Biophys Res Commun.* 1999; 257: 79–83. PMID: [10092513](#)
21. Schaffler A, Buechler C. CTRP family: linking immunity to metabolism. *Trends Endocrinol Metab.* 2012; 23: 194–204. doi: [10.1016/j.tem.2011.12.003](#) PMID: [22261190](#)
22. O'Shea KM, Chess DJ, Khairallah RJ, Hecker PA, Lei B, Walsh K, et al. Omega-3 polyunsaturated fatty acids prevent pressure overload-induced ventricular dilation and decrease in mitochondrial enzymes despite no change in adiponectin. *Lipids Health Dis.* 2010; 9: 95. doi: [10.1186/1476-511X-9-95](#) PMID: [20819225](#)
23. O'Shea KM, Chess DJ, Khairallah RJ, Rastogi S, Hecker PA, Sabbah HN, et al. Effects of adiponectin deficiency on structural and metabolic remodeling in mice subjected to pressure overload. *Am J Physiol Heart Circ Physiol.* 2010; 298: H1639–1645. doi: [10.1152/ajpheart.00957.2009](#) PMID: [20348222](#)
24. Yan W, Zhang H, Liu P, Wang H, Liu J, Gao C, et al. Impaired mitochondrial biogenesis due to dysfunctional adiponectin-AMPK-PGC-1alpha signaling contributing to increased vulnerability in diabetic heart. *Basic Res Cardiol.* 2013; 108: 329. doi: [10.1007/s00395-013-0329-1](#) PMID: [23460046](#)
25. Guo R, Zhang Y, Turdi S, Ren J. Adiponectin knockout accentuates high fat diet-induced obesity and cardiac dysfunction: role of autophagy. *Biochim Biophys Acta.* 2013; 1832: 1136–1148. doi: [10.1016/j.bbadis.2013.03.013](#) PMID: [23524376](#)
26. Ma K, Cabrero A, Saha PK, Kojima H, Li L, Chang BH, et al. Increased beta -oxidation but no insulin resistance or glucose intolerance in mice lacking adiponectin. *J Biol Chem.* 2002; 277: 34658–34661. PMID: [12151381](#)
27. Peterson JM, Wei Z, Seldin MM, Byerly MS, Aja S, Wong GW. CTRP9 transgenic mice are protected from diet-induced obesity and metabolic dysfunction. *Am J Physiol Regul Integr Comp Physiol.* 2013; 305: R522–533. doi: [10.1152/ajpregu.00110.2013](#) PMID: [23842676](#)
28. Zheng Q, Yuan Y, Yi W, Lau WB, Wang Y, Wang X, et al. C1q/TNF-related proteins, a family of novel adipokines, induce vascular relaxation through the adiponectin receptor-1/AMPK/eNOS/nitric oxide signaling pathway. *Arterioscler Thromb Vasc Biol.* 2011; 31: 2616–2623. doi: [10.1161/ATVBAHA.111.231050](#) PMID: [21836066](#)
29. Yi W, Sun Y, Yuan Y, Lau WB, Zheng Q, Wang X, et al. C1q/tumor necrosis factor-related protein-3, a newly identified adipokine, is a novel antiapoptotic, proangiogenic, and cardioprotective molecule in the ischemic mouse heart. *Circulation.* 2012; 125: 3159–3169. doi: [10.1161/CIRCULATIONAHA.112.099937](#) PMID: [22653084](#)
30. Nawrocki AR, Rajala MW, Tomas E, Pajvani UB, Saha AK, Trumbauer ME, et al. Mice lacking adiponectin show decreased hepatic insulin sensitivity and reduced responsiveness to peroxisome proliferator-activated receptor gamma agonists. *J Biol Chem.* 2006; 281(5): 2654–2660 PMID: [16326714](#)